Hindawi Publishing Corporation
International Journal of Chemical Engineering
Volume 2016, Article ID 4012967, 8 pages
http://dx.doi.org/10.1155/2016/4012967

Research Article

CO_2 Capture by Carbon Aerogel–Potassium Carbonate Nanocomposites

Guang Yang, Hongchao Luo, Tomonori Ohba, and Hirofumi Kanoh

Graduate School of Science, Chiba University, Chiba 263-8522, Japan

Correspondence should be addressed to Hirofumi Kanoh; kanoh@faculty.chiba-u.jp

Received 15 October 2015; Accepted 26 January 2016

Academic Editor: Alírio Rodrigues

Recently, various composites for reducing CO_2 emissions have been extensively studied. Because of their high sorption capacity and low cost, alkali metal carbonates are recognized as a potential candidate to capture CO_2 from flue gas under moist conditions. However, undesirable effects and characteristics such as high regeneration temperatures or the formation of byproducts lead to high energy costs associated with the desorption process and impede the application of these materials. In this study, we focused on the regeneration temperature of carbon aerogel–potassium carbonate (CA–KC) nanocomposites, where KC nanocrystals were formed in the mesopores of the CAs. We observed that the nanopore size of the original CA plays an important role in decreasing the regeneration temperature and in enhancing the CO_2 capture capacity. In particular, 7CA–KC, which was prepared from a CA with 7 nm pores, exhibited excellent performance, reducing the desorption temperature to 380 K and exhibiting a high CO_2 capture capacity of 13.0 mmol/g-K_2CO_3, which is higher than the theoretical value for K_2CO_3 under moist conditions.

1. Introduction

Carbon dioxide (CO_2) is the principal greenhouse gas. It has been continuously released into the environment through the burning of fossil fuels and has led to global warming and anthropogenic climate change, such as droughts, desertification, permafrost melt, inundation, rising sea levels, and ecosystem disruption, and it is expected to substantially affect the future of mankind. Although alternative energy sources have been extensively investigated, no single alternative source can satisfy global energy demands; fossil fuels are therefore expected to remain the primary energy resource for the next several decades because of their advantages of low cost and high energy density. The atmospheric CO_2 concentration was 384 ppm in 2007 and is expected to reach 550 ppm by 2050; hence, mitigating the atmospheric CO_2 concentration is critical for protecting our environment [1, 2]. With both high CO_2 capture capacity and low cost, alkali metal carbonates (M_2CO_3, M = K, Na) have been recognized as potential sorbents for CO_2 sorption according to the following reaction [3]:

$$M_2CO_3\,(s) + H_2O\,(g) + CO_2\,(g) \rightleftarrows 2MHCO_3\,(s) \quad (1)$$

The forward reaction is a bicarbonate formation reaction (the theoretical CO_2 capture capacity is 7.24 mmol-CO_2/g-K_2CO_3), whereas the reverse reaction is an endothermic regeneration process that begins at 445.3 K and ends at 548.1 K when the heating rate is 20 K/min [4]. Thus, by using alkali metal carbonates, it is possible to selectively sorb CO_2 under a moist condition, which usually lowers CO_2 capacity of conventional physical adsorbents.

In recent years, to solve problems such as the slow reaction rate of bicarbonate formation and high energy consumption during regeneration, researchers have extensively investigated various composites containing alkali metal carbonates [5–8]. The regeneration behaviors of alkali metal carbonates change when they are supported on nanoporous structural materials such as activated carbon, Al_2O_3, or carbon nanofibers or when they are combined with MgO, TiO, or FeOOH, which can themselves capture CO_2. Because of the antagonistic relationship between the effects of high regeneration temperatures and low capture capacities, suitable materials have not been developed. Zhao et al. reported that K_2CO_3 sorbents exhibit better CO_2 capture performance than Na_2CO_3 sorbents and that the selection of a support material with appropriate characteristics is important

for carbonation and regeneration [9]. We also previously reported a detailed reaction mechanism for CO_2 occlusion by K_2CO_3 under moist conditions [10, 11]. Therefore, in the present study, we focus on impregnating K_2CO_3 into the nanopores of carbon aerogels (CAs) prepared by pyrolysis of a dried organic aerogel followed by carbonation, leading to the formation of vitreous black monoliths with highly cross-linked micropores and mesopores [12, 13]. The CAs provide a suitable mesoporous reaction field for forming K_2CO_3 nanocrystals because the CAs' surface area, pore structure, and size are easily controlled through manipulation of the molar ratios among reagents or the pH [14, 15]. In the present paper, the CO_2 capture ability of K_2CO_3 nanocrystals incorporated into mesopores of CAs is studied from the viewpoint of lowering the regeneration temperature while achieving high selectivity and high capture capacity.

2. Experimental Section

2.1. Preparation of CA. All reagents were purchased from Wako Pure Chemical Industries, Ltd. Resorcinol–formaldehyde (RF) solutions were synthesized under the following experimental conditions. The resorcinol-to-sodium carbonate (R/C) and resorcinol-to-formaldehyde (R/F) molar ratios were fixed at 500 and 0.5, respectively, and the molar ratio of resorcinol to deionized water (R/W) was varied among 0.14, 0.28, and 0.7 to produce RF gels with different pore sizes. For a given R/W ratio, the required resorcinol was weighed out and added to deionized water; the resulting mixture was then stirred until the resorcinol was completely dissolved. Formaldehyde and sodium carbonate were added to the mixture, resulting in yellowish homogeneous RF solutions that were subsequently sealed and placed in a thermostated bath at 303 K for 2 weeks for polymerization [12].

Water entrained within the gel network of the polymer was removed through solvent exchange; the gel was successively soaked in mixed solutions of acetone and water at a ratio of 1 : 1 and 3 : 1 and in pure acetone for 15 min each. Finally, the gel was immersed in acetone for 1 day at room temperature. To preserve the structure of the nanoporous material, the wet gel was dried using a supercritical drying process. The wet gel was then placed in a supercritical drying chamber, and CO_2 was slowly introduced to bleed the air from the chamber. CO_2 was introduced to a pressure of 10 MPa at 318 K and was maintained at this temperature for 3 h. Carbonization of the organic aerogels was conducted at 1173 K for 3 h under Ar flowing at 100 cm^3/min. As described later, the porosities of the three different CAs were characterized by N_2 gas adsorption measurements at 77 K; the three CAs were observed to have pore widths of 7, 16, and 18 nm; these CAs are denoted as 7CA, 16CA, and 18CA, respectively.

2.2. Preparation of CA–Potassium Carbonate (KC) Nanocomposites. CA–KC nanocomposites were prepared by impregnating the nanopores of the CAs with a 0.15 mol/dm^3 K_2CO_3 (99.5% chemical purity) aqueous solution [3]. The mixture was then stirred with a magnetic stirrer for 24 h at room temperature. The aqueous solution was dried at 378 K in a vacuum evaporator. The samples were subsequently dried again in a furnace under an Ar ambient atmosphere at 573 K for 2 h. The nanocomposites are denoted as xCA–KC, where x represents the pore width of the CAs.

2.3. Measurements and Characterization. The porosities of the CAs and the xCA–KC nanocomposites were characterized by N_2 adsorption at 77 K using an Autosorb-MP1 (Quantachrome Instruments). CO_2 adsorption was measured using a Belsorp-Mini (MicrotracBEL Corp.). The CA and xCA–KC nanocomposites were pretreated by heating to 423 K under vacuum for 2 h before the gas adsorption measurements because K_2CO_3 is partially converted into $KHCO_3$ under an ambient atmosphere containing CO_2 and H_2O. Water adsorption isotherms were obtained by a gravimetric method at 303 K; the equilibration time was 2 h.

The Brunauer-Emmett-Teller (BET) method was used to analyze the specific surface areas (S_{BET}) on the basis of linear plots over the relative pressure (P/P_0) range 0.05–0.35 for the N_2 adsorption isotherm data. The total volume (V_T) was obtained at a relative pressure of 0.99, and the Dubinin-Radushkevich equation was used to calculate the micropore volume (V_{mic}). The mesopore diameters (D_{mes}) were estimated by the Barrett-Joyner-Halenda method.

The amount of K_2CO_3 impregnated into the mesopores of CA was determined by thermogravimetry-differential thermal analysis (TG-DTA, Shimadzu DTG-60AH), where the samples were heated to 1073 K. Because the residue consisted of K_2CO_3, the impregnated amounts of K_2CO_3 were calculated on the basis of the final TG curves to be 18.5, 21.3, and 18.8 wt% for 7CA–KC, 16CA–KC, and 18CA–KC, respectively, as shown in Figure S-1 (Supporting Information in Supplementary Material available online at http://dx.doi.org/10.1155/2016/4012967).

After the xCA–KC nanocomposites were heated to 473 K at 10 K/min under an N_2 atmosphere and maintained at 473 K for 5 min to ensure complete formation of K_2CO_3, the temperature was decreased to 313 K, and CO_2 and H_2O were introduced into the sample chamber of the TG–DTA apparatus for 2 h by flowing CO_2 through distilled water. The xCA–KC nanocomposites reacted with CO_2 and H_2O to form xCA–$KHCO_3$. The crystal structures before and after the CO_2 capture were measured through ex situ X-ray diffraction (XRD) on an X-ray diffractometer (MAC Science, M03XHF) equipped with a Cu $K\alpha$ radiation source (40 kV, 25 mA, and $\lambda = 0.15406$ nm). We heated the xCA–$KHCO_3$ nanocomposites to 473 K in order to study the regeneration process under the same conditions used in the aforementioned experiments.

We used the CaO solution-precipitation method to accurately determine the amount of CO_2 captured by the xCA–KC samples. The CaO solution was prepared by dissolving 0.6 g of CaO in 100 cm^3 distilled water. Any insoluble precipitate was filtered to yield a saturated solution. The clear solution was bubbled with N_2 gas to remove any dissolved CO_2 from air. The nanocomposites, which captured CO_2 under moist conditions in the TG–DTA chamber at 313 K, were heated at 573 K, and the desorbed CO_2 was recaptured by

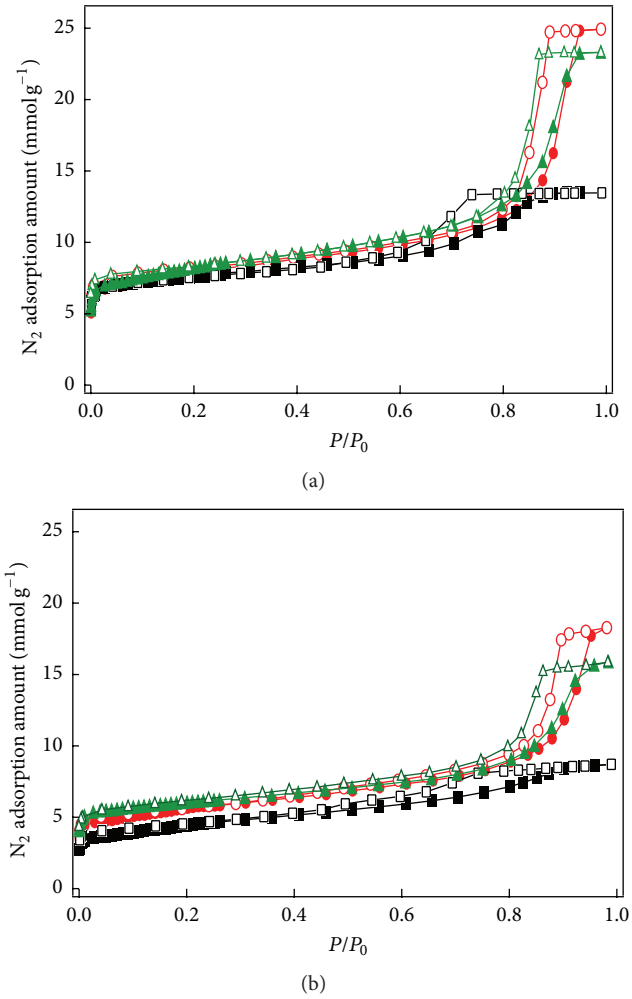

Figure 1: N_2 adsorption isotherms of (a) CAs and (b) *x*CA–KC samples at 77 K. Pore widths: black, 7 nm; green, 16 nm; red, 18 nm.

the CaO solution, leading to the immediate formation of a white precipitate. XRD analysis indicated that the precipitate was $CaCO_3$. Before the *x*CA–KC experiments, the reliability of the CaO solution-precipitation method was evaluated using analytical grade $KHCO_3$ powder, which indicated 92% precision with respect to the theoretical value.

3. Results and Discussion

3.1. BET Surface Area and Pore Size Distributions (PSDs) of the CAs and xCA–KCs. The pore structures were characterized using N_2 adsorption isotherms volumetrically measured at 77 K after pretreatment at 423 K for 2 h; the obtained isotherms are presented in Figure 1. The isotherms of the composites are categorized as type IV (IUPAC classification) with hysteresis between the adsorption and desorption branches. These isotherms indicate the presence of mesopores, although the increased adsorption at low relative pressures also indicates the presence of micropores. Zhao et al. examined the effects of the pore structure of Al_2O_3 supports on the ability of K_2CO_3 to capture CO_2 and observed that

Table 1: Pore parameters of the *x*CA and *x*CA–KC samples.

	S_{BET} (m^2/g)	V_T (cm^3/g)	V_{mic} (cm^3/g)	D_{mes} (nm)
7CA	517	0.43	0.25	7.0
7CA–KC	357	0.30	0.14	4.0
16CA	635	0.75	0.29	16
16CA–KC	459	0.55	0.20	12
18CA	523	0.88	0.24	18
18CA–KC	457	0.63	0.18	14

K_2CO_3 could quickly convert to $K_2CO_3{\cdot}1.5H_2O$ because of the mesoporous structure of the Al_2O_3 support [8]; they also observed that the micropores of the Al_2O_3 support facilitated the rapid conversion of $K_2CO_3{\cdot}1.5H_2O$ to $KHCO_3$. Thus, mesoporous structures can enhance CO_2 adsorption [8]. In the present study, the N_2 adsorption amount decreased for all samples after they were subjected to the K_2CO_3 impregnation treatment, indicating that K_2CO_3 was successfully incorporated into the micropores and mesopores of the CAs.

The pore structure parameters are compiled in Table 1, which shows that the surface area and pore volume of the *x*CA–KC nanocomposites decreased compared with those of the original CAs; this is consistent with the results of N_2 adsorption isotherms, which indicate a partial filling or blocking of the pores by impregnated K_2CO_3 [6]. The results in Table 1 indicate that 16CA possessed the highest surface area and exhibited the greatest decrease in surface area after the K_2CO_3 impregnation. This is in agreement with the result that 16CA–KC contained a larger amount of impregnated K_2CO_3 compared with the other *x*CA–KCs.

3.2. Structural Changes Induced by CO_2 Capture and Regeneration. The structural changes of the *x*CA–KCs that accompanied CO_2 capture and regeneration (the reverse reaction), which are represented as reaction (1) in Introduction, were examined by XRD analysis, as shown in Figure 2. Figure 2(a) shows the XRD patterns of the *x*CA–KC nanocomposites after the CO_2 capture under moist conditions. The main diffraction peaks of $KHCO_3$ are present, verifying that the $KHCO_3$ nanocrystals were introduced into the mesopores of the *x*CAs through the impregnation process. Although peaks attributable to $K_4H_2(CO_3)_3{\cdot}1.5H_2O$ as well as to $KHCO_3$ were observed in the patterns of 16CA–KC and 18CA–KC, all the peaks in the pattern of 7CA–KC were assigned to $KHCO_3$. The patterns in Figure 2(b) indicate almost complete regeneration because most of the main peaks were assigned to $K_2CO_3{\cdot}1.5H_2O$ instead of $KHCO_3$. This suggests that K_2CO_3 was formed by heat treatment at 473 K. Although $K_2CO_3{\cdot}1.5H_2O$ could be formed because of the deliquescent nature of K_2CO_3 under ambient conditions during the ex situ XRD experiment, K_2CO_3 impregnated into the mesopores of *x*CAs was exposed to the ambient atmosphere and more easily reacted with atmospheric water.

3.3. Decomposition of xCA–KC Nanocomposites. The *x*CA–KC nanocomposites were regenerated by heating to 473 K

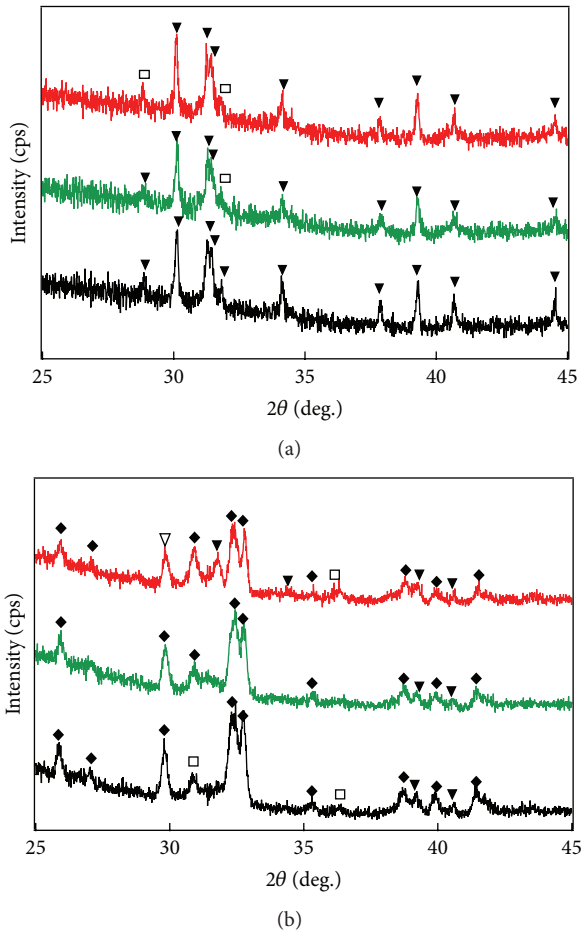

Figure 2: XRD patterns after CO_2 capture and regeneration: (a) xCA–KC nanocomposite after CO_2 capture under moist conditions; (b) xCA–KC nanocomposites placed under ambient atmosphere after being regenerated at 473 K for 2 h. Pore width: black, 7 nm; green, 16 nm; red, 18 nm. ▼: $KHCO_3$, □: $K_4H_2(CO_3)_3{\cdot}1.5H_2O$, ▽: K_2CO_3, and ◆: $K_2CO_3{\cdot}1.5H_2O$.

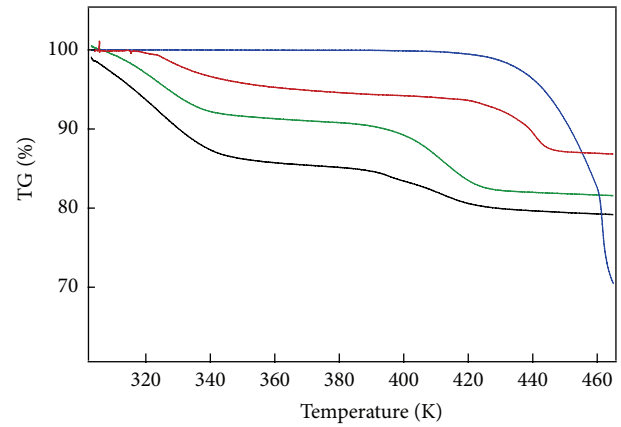

Figure 3: TG curves for the nanocomposites. Blue: $KHCO_3$, black: 7CA–KC, green: 16CA–KC, and red: 18CA–KC.

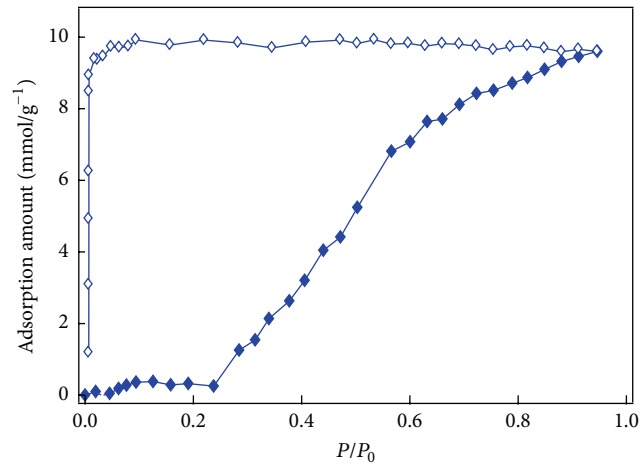

Figure 4: Water adsorption isotherms for K_2CO_3. Filled symbols: sorption; open symbols: desorption.

under an N_2 atmosphere. The changes in weight and temperature are shown in Figure 3; these results reflect characteristic thermal decomposition. In the TG traces of the xCA–KCs, the first weight loss is attributed to the desorption of water and the second is attributed to the decomposition of $KHCO_3$ to K_2CO_3, which is accompanied by the evolution of CO_2 and H_2O. The blue line shows the decomposition process of bulk $KHCO_3$, which began to decompose at >423 K. By contrast, the xCA–KCs clearly decomposed at lower temperatures with decreasing pore size of the original CAs: the decomposition onset temperature decreased to 420, 390, and 380 K for 18CA–KC, 16CA–KC, and 7CA–KC, respectively. Thus, 7CA–KC exhibits an effective decrease in the required regeneration temperature. We concluded that nanocrystals of K_2CO_3 impregnated into the nanopores of CA exhibited high reactivity, resulting in easier regeneration at lower temperatures. The regeneration temperature for 7CA–KC is lower than that for other potassium-based sorbents, and the regeneration behaviors are changed when K_2CO_3 is loaded onto different sorbents, mainly depending on the properties of the support material [16].

3.4. Water Adsorption. Water adsorption analysis is important for the xCA–KC nanocomposites because K_2CO_3 sorbs water from the ambient atmosphere. Zhao et al. reported that even though K_2CO_3–silica gel (SG) exhibits a relatively high pore volume, the total CO_2 sorption is only 34.5% because of the strong hygroscopicity of SG, easily leading to hydration of K_2CO_3 to $K_2CO_3{\cdot}1.5H_2O$ [8, 17]. This hydration should influence the CO_2-sorption amount of K_2CO_3 under moist conditions [18]. Because the CO_2 capture process of xCA–KCs involves both occlusion and physical adsorption, understanding the effects of water on CO_2 sorption of the original CA and the xCA–KCs is important. Figure 4 shows water sorption isotherms of K_2CO_3 at 303 K. Almost no water was adsorbed below a relative pressure P/P_0 of 0.2, whereas the sorption amount increased with increasing pressure and reached a maximum value of 9.6 mmol/g, corresponding to the water content in $K_2CO_3{\cdot}1.5H_2O$ (10.9 mmol/g).

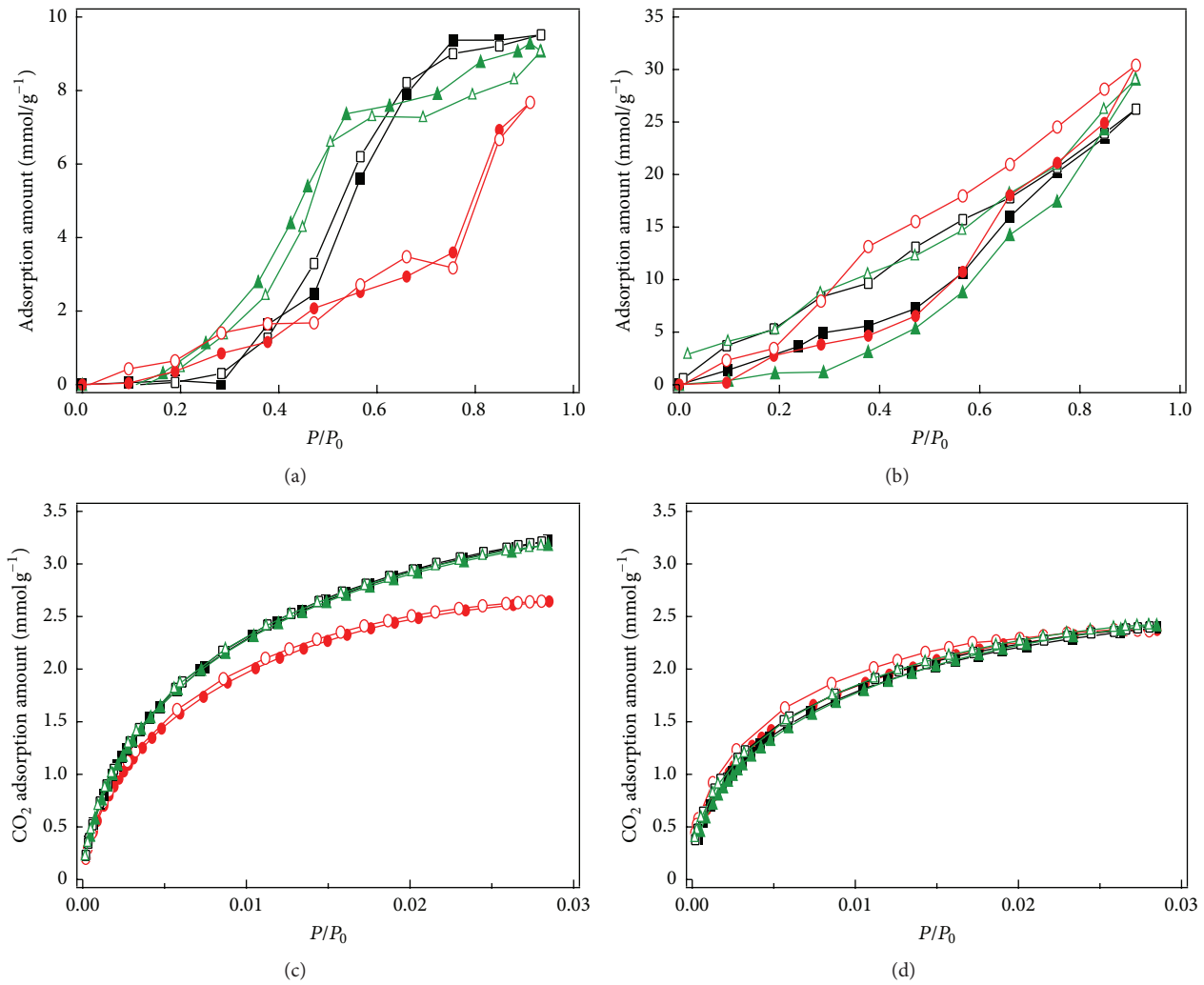

FIGURE 5: Water sorption and CO_2 sorption isotherms. Water sorption isotherms at 303 K for CAs (a) and *x*CA–KCs (b). CO_2 adsorption isotherms at 273 K under dry conditions for CA (c) and for *x*CA–KCs (d). Pore widths: black □, 7 nm; green △, 16 nm; red ○, 18 nm.

The desorption did not return to the original point because $K_2CO_3{\cdot}1.5H_2O$ hardly releases water molecules at ambient temperature, as demonstrated in the XRD experiments (Figure 2). Such a large hysteresis is likely observed because the hydrate formation from K_2CO_3 to $K_2CO_3{\cdot}1.5H_2O$ is extremely slow.

The water sorption isotherms of the CAs and *x*CA–KCs differ from those of K_2CO_3, as shown in Figure 5. Because the CAs are less hydrophilic than K_2CO_3, the physical adsorption of water is attributed to the micropores of the CAs [19]; thus, the three CAs should exhibit water uptake amounts corresponding to their micropore volume, as indicated in Figures 1(a) and 5(a) and in Table 1. The desorption isotherms did not exhibit adsorption hysteresis; they returned to the starting point reversibly, as shown in Figure 5(a).

By contrast, the water sorption behavior of the *x*CA–KCs was more complicated because both hydration of K_2CO_3 and physical adsorption by the micropores of the nanocomposites contributed to water sorption. Figure 5(b) shows remarkable increases in the water sorption uptakes of the *x*CA–KCs in the high relative pressure region. Notably, the amounts of sorbed water were greater than the sum of the water sorption amounts of K_2CO_3 and CAs. This phenomenon may be attributable to the nanocrystals of K_2CO_3 incorporated into nanopores of the CAs being more reactive and deliquescent under high humidity conditions than bulk K_2CO_3. The CO_2 sorption isotherms of the CAs and *x*CA–KCs are shown in Figures 5(c) and 5(d), respectively. Because of their diminished pore volumes, all the nanocomposites exhibited smaller CO_2 uptake after K_2CO_3 impregnation, and all the *x*CA–KCs exhibited a CO_2 capture capacity of approximately 2.4 mmol CO_2/g-sorbent at 0.1 MPa. Thus, the *x*CA–KCs do not exhibit good CO_2 capture ability under dry conditions.

3.5. CO_2 Capture Ability under Moist Conditions. The CO_2 sorption capacity of the *x*CA–KCs was calculated on the basis of their mass change resulting from reaction (1): one mole of K_2CO_3 occludes a stoichiometric amount of one mole of each of CO_2 and H_2O, and the two values were calculated as the total CO_2 sorption capacity (A_C; mmol-CO_2/g-sorbent)

and the CO_2 occlusion capacity of K_2CO_3 (R_C; mmol-CO_2/g-K_2CO_3). They are denoted as

$$A_C = \frac{1000nM_{CO_2}}{44m}, \qquad R_C = \frac{A_C}{\alpha}, \tag{2}$$

where n (mmol) is the total amount of CO_2 captured, as obtained from TG data; M_{CO_2} (g/mol) is the molar mass of CO_2; m (g) is the mass of the sorbent; and α is the impregnation rate of K_2CO_3 into the nanocomposites.

CO_2 sorption was conducted at 313 K at a flow rate of 100 cm^3/min in a saturated mixed gas of CO_2 and water, as shown in Figure 6. The increase in weight (%) corresponds to the conversion of K_2CO_3 to $2KHCO_3$. Sample 7CA–KC exhibited the greatest weight change (~17%), and bicarbonate formation reached equilibrium after 30 min for all the xCA–KC nanocomposites. Green et al. [20] reported that K_2CO_3 exhibits 45% CO_2 sorption in 100 min, and Luo et al. [11] verified that the carbonation of K_2CO_3 is low. The reaction rate of the xCA–KC nanocomposites was faster than that of bulk K_2CO_3, indicating the effect of nanostructured K_2CO_3.

The CO_2 capture capacity results are summarized in Table 2; the results indicate that 7CA–KC exhibits the highest CO_2 sorption capacity, A_C = 2.68 mmol/g-sorbent (R_C = 14.5 mmol/g-K_2CO_3), which is substantially higher than the theoretical amount of 7.24 mmol/g-K_2CO_3. The capture capacity results reported in Table 2 were estimated simply from the weight increase attributed to the sorption of CO_2 and H_2O. However, the mechanism is complicated and still under study. To more precisely determine the amount of CO_2 captured by the xCA–KC nanocomposites, we used another method to measure the net amount of CO_2 captured, as described in Section 3.6.

3.6. CaO Solution-Precipitation Method. To accurately determine the amount of CO_2 captured by the xCA–KC composites, the CaO solution-precipitation method described in experimental Section 2.3 was used. We measured the mass of the $CaCO_3$ precipitate to estimate the CO_2 uptake; the results indicated sorption capacities of A_C = 2.45, 2.1, and 1.7 and occlusion capacity of R_C = 13.0, 9.77, and 9.18 mmol/g-K_2CO_3 for 7CA–K_2CO_3, 16CA–K_2CO_3, and 18CA–K_2CO_3, respectively, which is also reported in Table 2. Although the amounts of CO_2 uptake are lower than those obtained from the TG measurements, these are net values of CO_2 capture capacity. Because the impregnated amount is insufficient, A_C is relatively low. If the impregnation of K_2CO_3 into the mesopores of CA can be improved, more CO_2 will be captured and the sorbents will be easily regenerated. The values of A_C and R_C exhibit a dependence on the pore size of the original CA. In the case of impregnation of 7 nm mesopores of CA, a higher value of A_C (per g-sorbent) is obtained. It may be because a smaller particle should be more reactive and show a higher efficiency for the CO_2 occlusion reaction with water vapor.

The CO_2 capture amounts are higher than the theoretical values in all xCA–KCs, as shown in Table 2. This can be because the remaining pores should be efficient for chemical absorption and physical adsorption of CO_2 such as the formation of H_2CO_3 in the pores (Figure S-2).

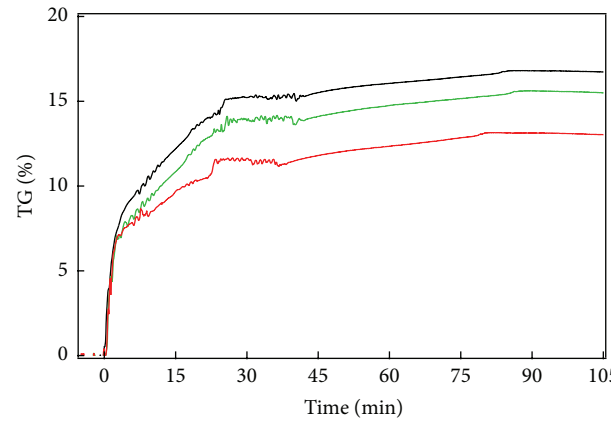

Figure 6: TG curves of carbonation reaction for xCA–KCs. Pore widths: black 7 nm; green 16 nm; red 18 nm.

The CO_2 capture amounts in the present study are excellent compared with those reported for other K_2CO_3-loaded composites [16, 21, 22]. Although dry potassium-based sorbents such as K_2CO_3–MgO exhibit excellent CO_2 capacities (9.0–14.9 mmol-CO_2/g-K_2CO_3) that are substantially higher than the theoretical value, these sorbents produce many other byproducts, leading to a higher temperature of 623 K for regeneration. Lee et al. [5, 21] reported that Al_2O_3–K_2CO_3 generates $KAl(CO_3)_2(OH)_2$ during the synthesis process and this byproduct does not completely convert to K_2CO_3 at temperatures below 563 K and observed that K_2CO_3–AC and K_2CO_3–TiO_2 can be regenerated at relatively low temperatures of 473 and 403 K, respectively. However, these two composites exhibit lower CO_2 capture capacities of 6.5 and 6.3 mmol-CO_2/g-K_2CO_3, respectively. AC–K_2CO_3 is considered a promising CO_2 capture sorbent because of its low regeneration energy requirement and high CO_2 capture capacity. However, to maintain these features, H_2O activation is required to convert K_2CO_3 to an activated form (K_2CO_3·1.5H_2O) [18]. ZrO_2–K_2CO_3 has a capacity of 6.2–6.9 mmol-CO_2/g-K_2CO_3 when the reaction temperature is within 323–333 K under an ambient atmosphere of 9% H_2O, 1% CO_2, and balance N_2 [5, 23].

4. Conclusion

CA–K_2CO_3 nanocomposites (xCA–KC) were prepared by impregnation of K_2CO_3 nanocrystals into the mesopores of three CAs with different pore sizes of 7, 16, and 18 nm for the development of an excellent CO_2 sorbent with a high capacity, high selectivity, and low energy cost for regeneration. The performance of the nanocomposites is attributed to both chemical and physical capture being involved in the CO_2 capture. The xCA–KCs can be completely regenerated at temperatures below 423 K; 7CA–K_2CO_3 in particular exhibited excellent results, where regeneration began at 380 K and was completed at 420 K. These results were attributed to the

Table 2: CO_2 capture capacity, as measured by TG–DTA and CaO soln–ppt method.

Composite	Loading amount	TG–DTA		CaO soln–ppt	
		A_C	R_C	A_C	R_C
7CA–K_2CO_3	18.5 wt%	2.68 (118)	14.5 (638)	2.45 (106)	13.0 (574)
16CA–K_2CO_3	21.3 wt%	2.45 (106)	11.4 (500)	2.1 (91)	9.77 (430)
18CA–K_2CO_3	18.8 wt%	2.1 (92)	11.1 (489)	1.7 (76)	9.18 (404)

A_C: mmol-CO_2/g-sorbent; (A_C): mg-CO_2/g-sorbent.
R_C: mmol-CO_2/g-K_2CO_3; (R_C): mg-CO_2/g-K_2CO_3.

high reactivity of nanostructured K_2CO_3, which rendered the K_2CO_3 crystals unstable and reduced the regeneration temperature. These *x*CA–KC nanocomposites exhibited excellent CO_2 capture capacity and can be considered a promising material for CO_2 capture from the viewpoints of economic effectiveness and energy efficiency. We also concluded that CAs can be used as a porous support for the preparation of nanocomposites with low sorbent regeneration temperatures.

Conflict of Interests

The authors declare that there is no conflict of interests regarding the publication of this paper.

Acknowledgments

This work was supported by the Iwatani Naoji Foundation's research grant and a Grant-in-Aid for Scientific Research from the Ministry of Education, Culture, Sports, Science and Technology (Japan). The authors would like to thank Enago (http://www.enago.jp/) for the English language review.

References

[1] J. Wang, L. Huang, R. Yang et al., "Recent advances in solid sorbents for CO_2 capture and new development trends," *Energy and Environmental Science*, vol. 7, no. 11, pp. 3478–3518, 2014.

[2] Q. Wang, J. Luo, Z. Zhong, and A. Borgna, "CO_2 capture by solid adsorbents and their applications: current status and new trends," *Energy and Environmental Science*, vol. 4, no. 1, pp. 42–55, 2011.

[3] S. C. Lee, Y. M. Kwon, C. Y. Ryu et al., "Development of new alumina-modified sorbents for CO_2 sorption and regeneration at temperatures below 200°C," *Fuel*, vol. 90, no. 4, pp. 1465–1470, 2011.

[4] S.-W. Park, D.-H. Sung, B.-S. Choi, J.-W. Lee, and H. Kumazawa, "Carbonation kinetics of potassium carbonate by carbon dioxide," *Journal of Industrial and Engineering Chemistry*, vol. 12, no. 4, pp. 522–530, 2006.

[5] S. C. Lee and J. C. Kim, "Dry potassium-based sorbents for CO_2 capture," *Catalysis Surveys from Asia*, vol. 11, no. 4, pp. 171–185, 2007.

[6] N. N. A. H. Meis, A. M. Frey, J. H. Bitter, and K. P. De Jong, "Carbon nanofiber-supported K_2CO_3 as an efficient low-temperature regenerable CO_2 sorbent for post-combustion capture," *Industrial & Engineering Chemistry Research*, vol. 52, no. 36, pp. 12812–12818, 2013.

[7] B.-T. Zhang, M. Fan, and A. E. Bland, "CO_2 separation by a new solid K–Fe sorbent," *Energy & Fuels*, vol. 25, no. 4, pp. 1919–1925, 2011.

[8] C. Zhao, X. Chen, and C. Zhao, "CO_2 absorption using dry potassium-based sorbents with different supports," *Energy and Fuels*, vol. 23, no. 9, pp. 4683–4687, 2009.

[9] C. Zhao, X. Chen, and C. Zhao, "Carbonation and active-component-distribution behaviors of several potassium-based sorbents," *Industrial & Engineering Chemistry Research*, vol. 50, no. 8, pp. 4464–4470, 2011.

[10] H. Chioyama, H. Luo, T. Ohba, and H. Kanoh, "Temperature-dependent double-step CO_2 occlusion of K_2CO_3 under moist conditions," *Adsorption Science & Technology*, vol. 33, no. 3, pp. 243–250, 2015.

[11] H. Luo, H. Chioyama, S. Thürmer, T. Ohba, and H. Kanoh, "Kinetics and structural changes in CO_2 capture of K_2CO_3 under a moist condition," *Energy & Fuels*, vol. 29, no. 7, pp. 4472–4478, 2015.

[12] R. W. Pekala, "Organic aerogels from the polycondensation of resorcinol with formaldehyde," *Journal of Materials Science*, vol. 24, no. 9, pp. 3221–3227, 1989.

[13] R. W. Pekala, C. T. Alviso, F. M. Kong, and S. S. Hulsey, "Aerogels derived from multifunctional organic monomers," *Journal of Non-Crystalline Solids*, vol. 145, pp. 90–98, 1992.

[14] S. J. Taylor, M. D. Haw, J. Sefcik, and A. J. Fletcher, "Gelation mechanism of resorcinol-formaldehyde gels investigated by dynamic light scattering," *Langmuir*, vol. 30, no. 34, pp. 10231–10240, 2014.

[15] D. Fairén-Jiménez, F. Carrasco-Marín, and C. Moreno-Castilla, "Porosity and surface area of monolithic carbon aerogels prepared using alkaline carbonates and organic acids as polymerization catalysts," *Carbon*, vol. 44, no. 11, pp. 2301–2307, 2006.

[16] C. Zhao, X. Chen, and C. Zhao, "K_2CO_3/Al_2O_3 for capturing CO_2 in flue gas from power plants. Part 2: regeneration behaviors of K_2CO_3/Al_2O_3," *Energy & Fuels*, vol. 26, no. 2, pp. 1406–1411, 2012.

[17] C. Zhao, X. Chen, E. J. Anthony et al., "Capturing CO_2 in flue gas from fossil fuel-fired power plants using dry regenerable alkali metal-based sorbent," *Progress in Energy and Combustion Science*, vol. 39, no. 6, pp. 515–534, 2013.

[18] C. Zhao, X. Chen, C. Zhao, and Y. Liu, "Carbonation and hydration characteristics of dry potassium-based sorbents for CO_2 capture," *Energy & Fuels*, vol. 23, no. 3, pp. 1766–1769, 2009.

[19] Y. Hanzawa and K. Kaneko, "Lack of a predominant adsorption of water vapor on carbon mesopores," *Langmuir*, vol. 13, no. 22, pp. 5802–5804, 1997.

[20] D. A. Green, B. S. Turk, J. W. Portzer et al., "Carbon dioxide capture from flue gas using dry regenerable sorbents," Quarterly Technical Progress Report, 2003.

[21] S. C. Lee, B. Y. Choi, T. J. Lee, C. K. Ryu, Y. S. Ahn, and J. C. Kim, "CO_2 absorption and regeneration of alkali metal-based solid sorbents," *Catalysis Today*, vol. 111, no. 3-4, pp. 385–390, 2006.

[22] C. L. Soo, J. C. Ho, J. L. Soo et al., "Development of regenerable MgO-based sorbent promoted with K_2CO_3 for CO_2 capture at low temperatures," *Environmental Science & Technology*, vol. 42, no. 8, pp. 2736–2741, 2008.

[23] S. C. Lee, H. J. Chae, S. J. Lee et al., "Novel regenerable potassium-based dry sorbents for CO_2 capture at low temperatures," *Journal of Molecular Catalysis B: Enzymatic*, vol. 56, no. 2-3, pp. 179–184, 2009.